Front. Earth Sci. 2018, 12(1): 134–147
https://doi.org/10.1007/s11707-017-0625-4

RESEARCH ARTICLE

Clay mineralogy and its palaeoclimatic significance in the Luochuan loess-palaeosols over ~1.3 Ma, Shaanxi, northwestern China

Changdok WON[1,2], Hanlie HONG (✉)[1,3], Feng CHENG[1], Qian FANG[1], Chaowen WANG[4], Lulu ZHAO[1], Gordon Jock CHURCHMAN[5]

1 School of Earth Sciences, China University of Geosciences, Wuhan 430074, China
2 Kim Chaek University of Technology, Pyongyang 999093, D.P.R of Korea
3 State Key Laboratory of Biogeology and Environmental Geology, China University of Geosciences (Wuhan), Wuhan 430074, China
4 Gemological Institute, China University of Geosciences (Wuhan), Wuhan 430074, China
5 School of Agriculture, Food and Wine, The University of Adelaide, Adelaide SA5005, Australia

Abstract To understand climate changes recorded in the Luochuan loess-palaeosols, Shaanxi province, northwestern China, clay mineralogy was studied using X-ray diffraction (XRD), high-resolution transmission electron microscopy (HRTEM), and scanning electron microscopy (SEM) methods. XRD results show that clay mineral compositions in the Luochuan loess-palaeosols are dominantly illite, with minor chlorite, kaolinite, smectite, and illite-smectite mixed-layer clays (I/S). Illite is the most abundant species in the sediments, with a content of 61%–83%. The content of chlorite ranges from 5%–22%, and the content of kaolinite ranges from 5%–19%. Smectite (or I/S) occurs discontinuously along the loess profile, with a content of 0–8%. The Kübler index of illite (IC) ranges from 0.255°–0.491°, and the illite chemical index (ICI) ranges from 0.294–0.394. The CIA values of the loess-palaeosols are 61.9–69.02, and the $R^{3+}/(R^{3+} + R^{2+} + M^{+})$ values are 0.508–0.589. HRTEM observations show that transformation of illite to illite-smectite has occurred in both the loess and palaeosol, suggesting that the Luochuan loess-palaeosols have experienced a certain degree of chemical weathering. The Luochuan loess-palaeosols have the same clay mineral assemblage along the profile. However, the relative contents of clay mineral species, CIA, ICI, and IC values fluctuate frequently along the profile, and all these parameters display a similar trend. Moreover, climate changes suggested by the clay index are consistent with variations in the deep-sea $\delta^{18}O$ records and the magnetic susceptibility value, and thus, climate changes in the Luochuan region have been controlled by global climate change.

Keywords clay minerals, weathering, palaeoclimate, Luochuan, loess-palaeosols

1 Introduction

Loess deposits blanket over ~10% of the globe, and are located near mountainous areas, desert margins and in alluvial plains of rivers (Ahmad and Chandra, 2013; Schatz et al., 2015). During interglacials and interstadials, when more humid and warmer climates prevailed, dust deposition weakened and environments favored soil formation (Schatz et al., 2015; Sun et al., 2016). The loess profile recorded the multicycle variation of bioclimatic environments of the China Loess Plateau (CLP) and even in Eurasia during the Quaternary, and thus have provided very useful materials for the study of palaeoclimate and palaeoenvironment (Buggle et al., 2011, 2014; Ahmad and Chandra, 2013; Terhorst et al., 2014; Yang et al., 2014; Schatz et al., 2015; Sun et al., 2015; Li et al., 2016). Paleoclimate investigations on these deposits mainly focused on palaeopedological indices such as grain size distributions, clay and iron mineralogy, geochemistry-based weathering proxies, and soil micromorphology (Buggle et al., 2011, 2014; Hu et al., 2013; Lu et al., 2015).

The Luochuan loess-palaeosol section is located in Luochuan county, Shaanxi province, northwestern China. It outcrops well and displays continuous loess-palaeosol sequences. The Luochuan loess section has been inten-

Received August 6, 2016; accepted October 16, 2016

E-mail: honghl8311@aliyun.com

sively investigated in recent years. Previous investigations focused mainly on particle size distribution, magnetic susceptibility, magnetic mineral composition, biomarkers, fixed ammonia, detrital zircon, and carbon isotope composition (Yuan et al., 1987; Lu et al., 1998; Rao et al., 2004; Yang et al., 2006; Zhang et al., 2007; Xie et al., 2008; Lu et al., 2008). However, fewer studies of clay mineralogy have been undertaken on the Luochuan section. Zheng et al. (1985) studied the relative changes of the clay contents and the palaeoclimate evolution for the loess profile in Luochuan and Longxi. Ji et al. (1997) and Chen et al. (2004) investigated the origin of clay minerals based on the crystallinity and morphology of illite. Ji et al. (1999) studied the relation between chemical weathering of chlorite and magnetic susceptibility of the Luochuan loess-palaeosols. However, discrepancies still exist in palaeoenvironment interpretations of the materials between different indicators.

The palaeosol deposits in the profile were formed by a certain degree of chemical weathering, resulting in mineral alteration and transformation. Multiple lines of evidence for climatic change are usually preserved in the clay components of deposits, since they are the most sensitive fractions of sediments. In this paper, we investigate the clay mineralogy of the Luochuan loess-palaeosol sequences, aiming to obtain greater understanding of clay transformation in the environment, and thus, to shed light on the use of clay mineral indices of loess-palaeosol sediments, and to enable a better interpretation of climatic changes from the materials.

2 Geological setting

The Luochuan section is situated at Heimugou village (35º42' 42"N and 109º25' 2"E), in the Luochuan Loess National Geopark, 5 km distance from the south of the Luochuan county (Fig. 1). It is located in the central part of the CLP and in the zone of the northern temperate continental wet and dry monsoon climate, with a mean annual temperature of ~12ºC and annual precipitation lower than evaporation capacity. The altitude is about 1135–1160 m, and it is one of regions in which the lithosphere thickness is less than 200 km. With good outcrops, completeness, and the stability of its loess-palaeosol sequences, the section is considered as the typical loess-palaeosol section of loess deposit in China.

The Luochuan section is composed of yellow to sallow silts or sandy clay soils (loess) and light brown silted clay soils (palaeosol) with loose and porous texture and

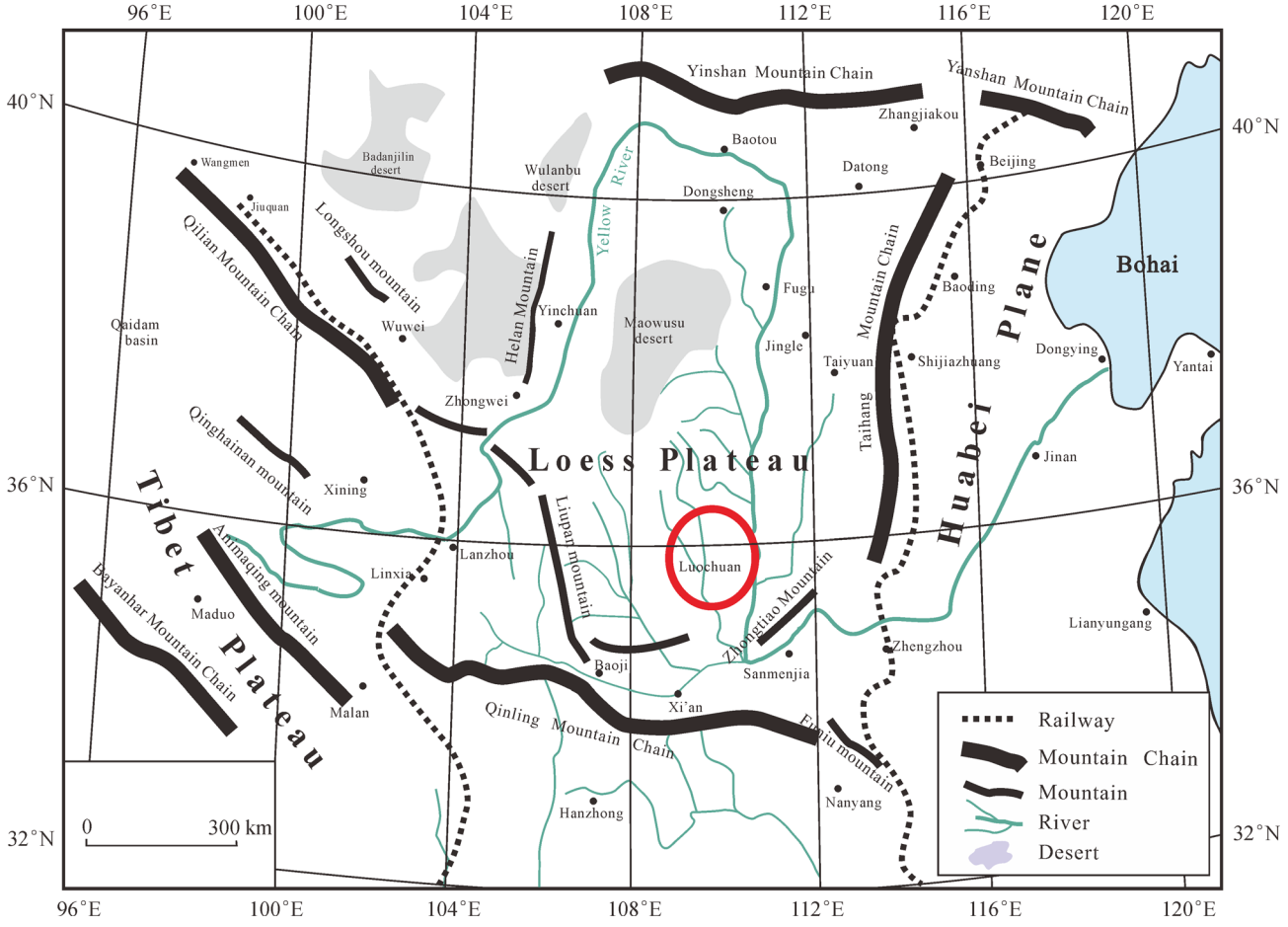

Fig. 1 Geographic location of the Luochuan loess-palaeosol profile.

calcareous concretions, in some cases having iron or manganic spots in loess layers. It unconformably overlays the sandstone of the Zidan group of the Lower Cretaceous. The red clay in the base of the section is about 8 m thick, with a lowest boundary age of 3.2 Ma. The section is about 140 m thick. The lithology of the profile is described in Fig. 2.

3 Materials and methods

3.1 Sampling and preparation

For detailed clay mineralogical analyses, the loess-palaeosol samples (~1 kg each) were collected from the Luochuan loess-palaeosol sequences of Pleistocene to Holocene age, at 20–70 cm intervals according to the lithology and layer thickness. A total of 224 samples were obtained and then investigated in the present study.

The bulk samples were dried at ambient temperature and were then ground manually to pass through a 200 mesh. The organic matter was removed by hydrogen peroxide (20% H_2O_2). The powder samples of 10–16 g were treated with a buffer solution of 0.1 mol/L dilute hydrochloric acid for decalcification, followed by washing with distilled water. The Fe oxides were extracted by the CBD method (Buggle et al., 2014). In order to obtain good dispersions, a 1% aqueous solution of sodium hexametaphosphate was added into the powder sample solution, which was then agitated until well dispersed (Andreola et al., 2004). The < 2 μm clay fraction was separated by a sedimentation method (Burt, 2004; Jaramillo et al., 2015). Oriented clay samples were prepared for XRD clay mineralogical determination by dropping the clay suspension onto glass slides and were then dried at the ambient temperature. For the determination of smectite and/or illite-smectite clays in the samples, oriented samples were saturated with ethylene glycol at 65ºC for 4 h in an electric oven (Rateev et al., 1969; Keller, 1970; Hong et al., 2008).

3.2 XRD analysis

X-ray diffraction was performed on a Panalytical X'Pert PRO DY2198 diffractometer with Ni-filtered Cu Kα radiation at 40 kV and 35 mA at the Key Laboratory of Geological Processes and Mineral Resources (GPMR) of China University of Geosciences (Wuhan). The slit conditions were: DS = SS = 1°, RS = 0.3 mm. The XRD profiles were recorded from 3° to 65° 2θ, with a scan rate of 4° 2θ/min.

Clay minerals were identified according to composite contrasts of XRD patterns of the air dried sample (N) and the ethylene-glycol (EG) solvated sample (Jaramillo et al., 2015). A 17 Å (001) peak in the XRD pattern of the ethylene-glycol (EG) solvated sample indicates the existence of smectite or irregular I/S mixed-layer clay. Illite is characterised by 10 Å, 5 Å, and 3.34 Å peaks, chlorite is identified by peaks for 14.2 Å, 7.1 Å, and 3.54 Å, and kaolinite is typified by 7.1 Å and 3.58 Å peaks in the XRD pattern of the EG sample. The relative contents of clay mineral species were semi-quantitatively estimated from the peak heights (Biscaye, 1965), which were then scaled and adjusted according to the following formula: 4×I (illite-10 Å) + I (smectite-17 Å) + 2×I (kaolinite, chlorite) = 100%, and the contents of kaolinite and chlorite were further determined according to intensities of the 002 reflection of kaolinite and the 004 reflection of chlorite. The crystallinity of illite (IC) was estimated from the full width at half maximum (FWHM) of the 001 reflection of illite; the greater the IC value, the lower the illite crystallinity (Kisch, 1991; Wang and Zhou, 1998; Hong et al., 2012a). Illite chemical index (ICI) was calculated from the ratio of 5.0 Å peak height to10 Å peak (Gingele et al., 2001; Xu et al., 2010).

3.3 SEM analysis

Small blocks of the selected bulk samples were cut to ~0.5 cm in diameter and were then gold-coated (Hong et al., 2007). Scanning electron microscope (SEM) analysis was undertaken at the GPMR of China University of Geosciences (Wuhan) on a JSM-5610 scanning electron microscope at 20 kV accelerating voltage and a beam current of 1–3 nA. The instrument was equipped with an energy-dispersive spectrometer (EDS) system, which can provide the chemical composition of a microscope zone and favor the determination of mineral particles during SEM observation.

3.4 HRTEM analysis

Representative loess and palaeosol samples from L15 and S14 layers were selected for high-resolution transmission electron microscopy (HRTEM) analysis, in order to investigate the alteration and transformation of clay minerals in the pedogenic processes. Some of the < 2 μm clay fraction was added into a small plastic tray with methanol, and was then dispersed using the ultrasonic equipment for 10 min. The well-dispersed clay particles were collected on a copper net and were further dried using an infrared light. HRTEM observations were undertaken at the GPMR of China University of Geosciences (Wuhan) on a JEM 2010FEF transmission electron microscope equipped with a Phoenix 60T EDS. The instrument was operated at 200 kV accelerating voltage.

4 Results

4.1 XRD results

The XRD profiles of representative clay fractions are

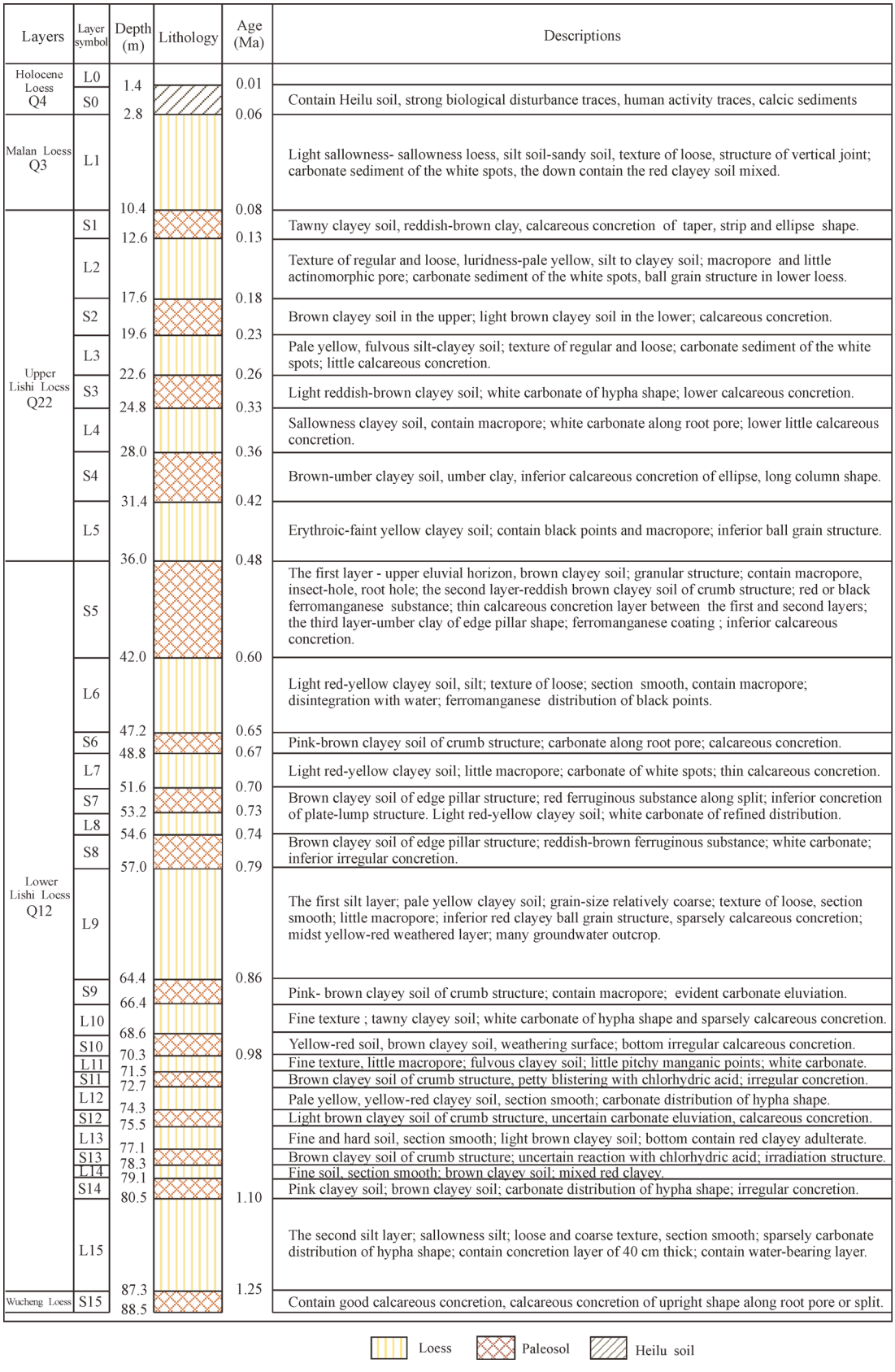

Fig. 2 Schematic diagram showing the lithology of the Luochuan section (ages from Sun and Liu, 2002).

shown in Fig. 3. Clay mineral components in the Luochuan loess and palaeosol samples are mainly illite, with minor chlorite, kaolinite, illite-smectite mixed-layer clays, and smectite. The illite content ranges from 61% to 83%, with an average value of 74%. Chlorite occurs abundantly in the loess and palaeosol sequences, with a content ranging from 6% to 22% and a mean value of 15%. Kaolinite is also present in the samples; the content of kaolinite ranges from 5% to 19% with an average value of 11%. In the Luochuan loess-palaeosol samples, illite-smectite mixed-layer clays usually have an 001 spacing of 12–15 Å, and overlap with that of smectite. After the glycol treatment, the 12–15 Å peak disappeared while the intensity of the 10 Å peak increased, suggesting that a mixed-layer I/S in Luochuan loess-palaeosol samples has a random stacking structure. Accordingly, the relative proportion of smectite estimated from the XRD pattern of glycolated samples included discrete smectite and the smectite component of mixed-layer I/S. Smectite occurs occasionally in layers of the loess-palaeosol profile, with a content ranging from 0 to 8% and an average value of 3%.

The content of illite is relatively stable in layers S0–L7; it varies only in a small range of 64%–82%. In the layers S7–S15, illite abundance changes with the lithology along the profile: the illite content is generally larger in the palaeosol layers (67%–83%) than those in the loess layers

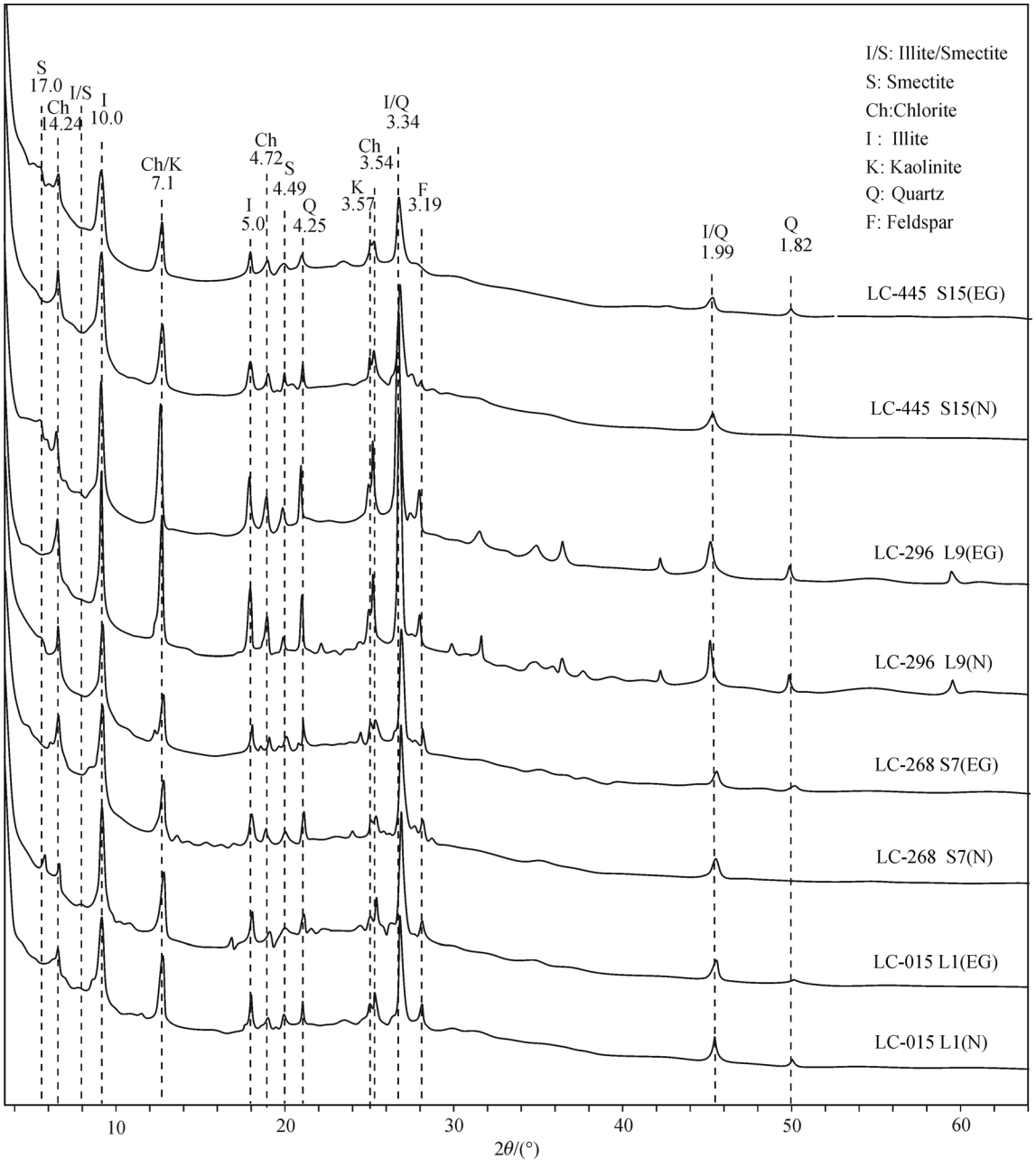

Fig. 3 XRD patterns of representative samples of clay fractions.

(61%–78%). The content of chlorite ranges from 6% to 21% in layers S0–L7; it shows no clear relation with lithology. However, in the layers S7–S15, chlorite abundance exhibits a close relation with lithology. The chlorite contents are generally larger in the loess layers (13%–22%) than in the palaeosol layers (6%–18%). The content of kaolinite changes from 5% to 19% in the loess-palaeosol profile; it shows no clear relation with lithology. Smectite appears discontinuously (0–8%) in the layers along the profile. However, the content of smectite is generally larger in palaeosols than in loesses.

The values of illite crystallinity range from 0.255° to 0.491°, with an average value of 0.36°. The values of the illite chemical index range from 0.294 to 0.394, with an average value of 0.319. Changes in illite crystallinity show a close relation with lithology along the profile. In general, the value of illite crystallinity is larger in the palaeosols (0.31°–0.491°) relative to those in the loesses (0.255°–0.401°). The change in the illite chemical index exhibits a similar trend to that of illite crystallinity; the value of the illite chemical index is generally larger in the palaeosols (0.299–0.394) than that in the loesses (0.294–0.334). Changes in clay mineral content, illite crystallinity, and illite chemical index along the loess-palaeosol profile are plotted in Fig. 4.

4.2 SEM observation

The loess-palaeosol sediments exhibit a loose texture under the SEM. However, the palaeosol sample shows a relatively condensed texture compared to that of the loess sample (Fig. 5). Clay mineral particles in the loess and palaeosol sediments appear as discrete flakes with angular to irregular morphology, and the clay aggregates in the palaeosol sample exhibit a typical swirly texture, in which clay mineral flakes show face to face arrangement. Smectite shows fleecy and honeycomb morphologies, with no preferred orientation (Figs. 5(a) and 5(b)). Illite exhibits curved and scalloped outlines, and is enriched in K compared to smectite (Fig. 5(c)). Under the SEM, most kaolinite is characterized by tiny booklet-like hexagonal morphology, although some particles show rounded shapes (Fig. 5(d)). Clay flakes generally exhibit ragged edges with poorly-developed lateral dimensions. Compared to the loess sample, clay grains usually display much smaller and thinner platy shapes, and some of the clay flakes were observed with rounded outlines, or with bay-shaped edges in the palaeosol sample, suggesting that clay particles in the palaeosol have undergone a certain degree of dissolution during weathering.

4.3 HRTEM observation

Various clay mineral morphologies are observed in HRTEM analysis. Most of the clay grains display straight outlines, and in the lattice fringe images the fringes are usually straight and all have a spacing of 10 Å, indicative of illitic minerals (Figs. 6(b), 6(c), 6(d) and 7(b)). Some of the clay particles exhibit a typical wavy shape, suggesting the presence of mixed-layer I/S clays, in agreement with the XRD results. Under HRTEM observation, the I/S flakes show interstratified lattice fringe images, the lattice spacings of 10 Å are usually interstratified with those of 12 or 15 Å. Some of the wave-shaped flakes appear to have only 12 Å layers, without interstratified 10 Å fringes, while in parts of the clay flakes, the lattice fringes consist of dominantly 10 Å layers with minor 12 Å layers. The 15 Å lattice fringe spacing of the smectite layer collapsed to 12 Å under the electron beam in HRTEM observation; the former are probably interpreted as smectite clay and the latter as mixed-layer I/S clays (Nieto et al., 1996). In most of the clay flakes, the illite/smectite interstratified sequences are disordered; the smectite layer is usually interstratified with different numbers of illite layers, indicating random stacking sequences.

5 Discussion

5.1 Characteristics of clay minerals in the loess-palaeosols

The clay mineral assemblages in sedimentary rocks usually contain both authigenic and detrital clay minerals (Singer, 1984). Detrital clay minerals record palaeoclimate information of the source area, while the authigenic clay minerals document the climate condition of the sedimentary area. The loess-palaeosol sequences have experienced the combined processes of sedimentation and pedogenic weathering. Although pedogenic alteration could probably remove some imprints which document the environmental and climatic conditions, the process could also form clay minerals in correspondence with the pedogenic conditions of the materials. Therefore, evidence for environmental and climatic conditions could probably be preserved in the clay component of the sediments (Perederij, 2001). The clay mineral composition of the Luochuan loess-palaeosols is mainly illite with minor illite-smectite mixed-layer clays, chlorite, and kaolinite, and trace smectite. HRTEM evidence shows that illite-smectite mixed-layer clays exhibit an irregular I/S stacking structure, regarded as an intermediate forming during the progressive alteration of illite to smectite under the supergene pedogenic conditions. Moreover, SEM observations show that clay mineral particles in the loess-palaeosols usually have angular and irregular outlines with ragged edges and poorly-developed lateral dimensions, indicating a detrital origin and dissolution due to weathering. Illite in the Luochuan loess-palaeosols is the species of the $2M_1$ illite polytype, as indicated by the XRD pattern.

The illite crystallinity of the loess-palaeosols ranges from 0.255° to 0.491°. The relatively lower illite crystallinity suggests that illite has experienced weathering or

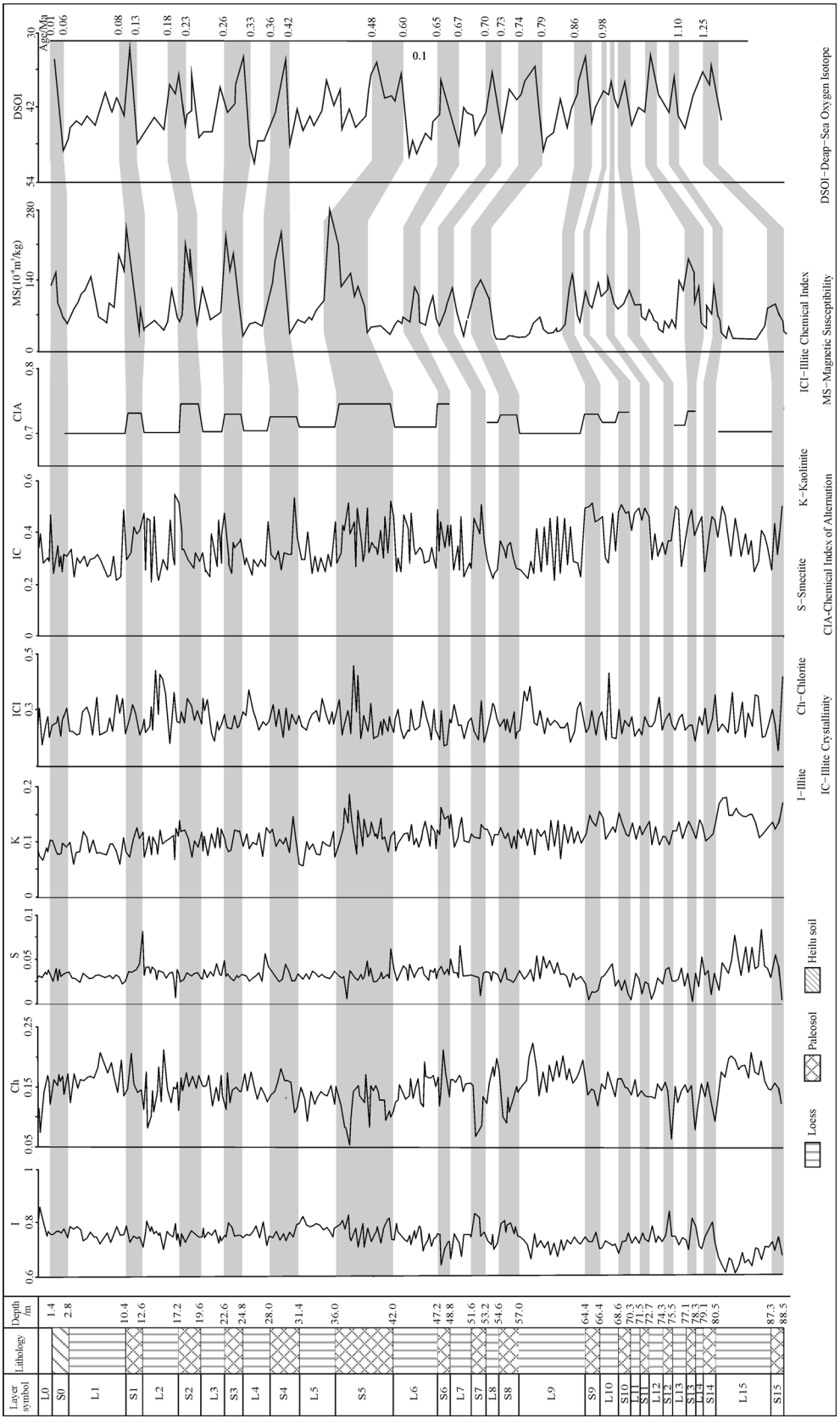

Fig. 4 Clay mineral feature curves of the Luochuan loess-palaeosol section and its correlation with magnetic susceptibility curves and the deep-sea oxygen isotope records (deep-sea oxygen isotope and magnetic susceptibility adapted from Sun and Liu, 2002).

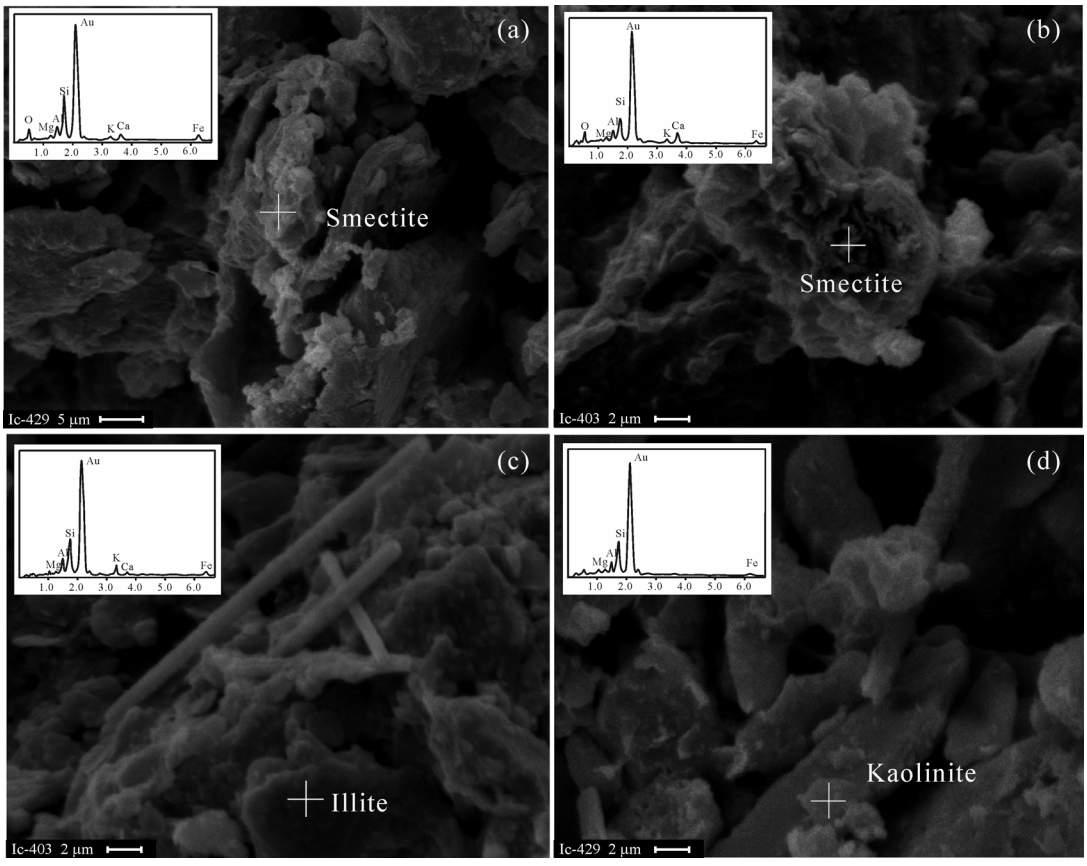

Fig. 5 SEM photos of the clay minerals in the loess (LC-429) and palaeosol (LC-403) in the Luochuan section. 1-lump shape clay mineral (LC-429), 2-bended schistose shape clay mineral(LC-403).

hydrolysis. Al-rich (muscovitic) illite has an illite chemical index value of > 0.4, while Fe- and Mg-rich (biotitic) illite has a value < 0.15; the former represents intensive hydrolysis and the latter represents the result of mechanical weathering (Petschick et al., 1996; Trindade et al., 2013). The illite chemical index values of the Luochuan loess-palaeosols range from 0.294 to 0.394, suggesting that illite in loess-palaeosols has experienced a certain degree of chemical weathering, consistent with the results of illite crystallinity. Chlorite is usually stable in the alkaline environment that inhibits chemical weathering. During the pedogenic process dominated by chemical weathering, the divalent iron within brucite layers is easily oxidized and thus chlorite would alter into kaolinite, and in strongly weathered laterite sediments chlorite would completely disappear after prolonged chemical weathering. Illite is usually considered as a little-altered clay species with a detrital origin. Thus, the clay minerals chlorite and illite are generally the dominant clay species when there is only weak chemical weathering, and the occurrence of chlorite and illite is indicative of cold climate conditions marked by very low rates of chemical weathering (Hallam et al., 1991).

Pedogenic smectite and illite-smectite clays are generally produced under moderate chemical weathering, and usually form in poorly-drained areas of low relief under seasonally warm/humid and dry tropical to subtropical climate conditions (Hong et al., 2007). Kaolinite is often considered as a pedogenic product; in a supergene weathering environment it is usually formed by the alteration of silicates in the presence of an acidic medium under conditions of strong leaching and a warm/humid climate. The presence of kaolinite, smectite, and mixed-layer illite/smectite clays throughout the Luochuan loess-palaeosols suggest a certain degree of chemical weathering occurred in the area and, therefore, variations in relative proportions in the clay mineral assemblage along the loess-palaeosol profile could be attributed to changing climate conditions.

5.2 Palaeoclimatic evolution as indicated by clay mineralogy

The XRD results of the clay fractions in the Luochuan section show that the loess-palaeosols have similar clay mineral compositions. However, illite crystallinity clearly shows differences between the loess and palaeosol layers. In the weathering process, K^+ will be liberated from the

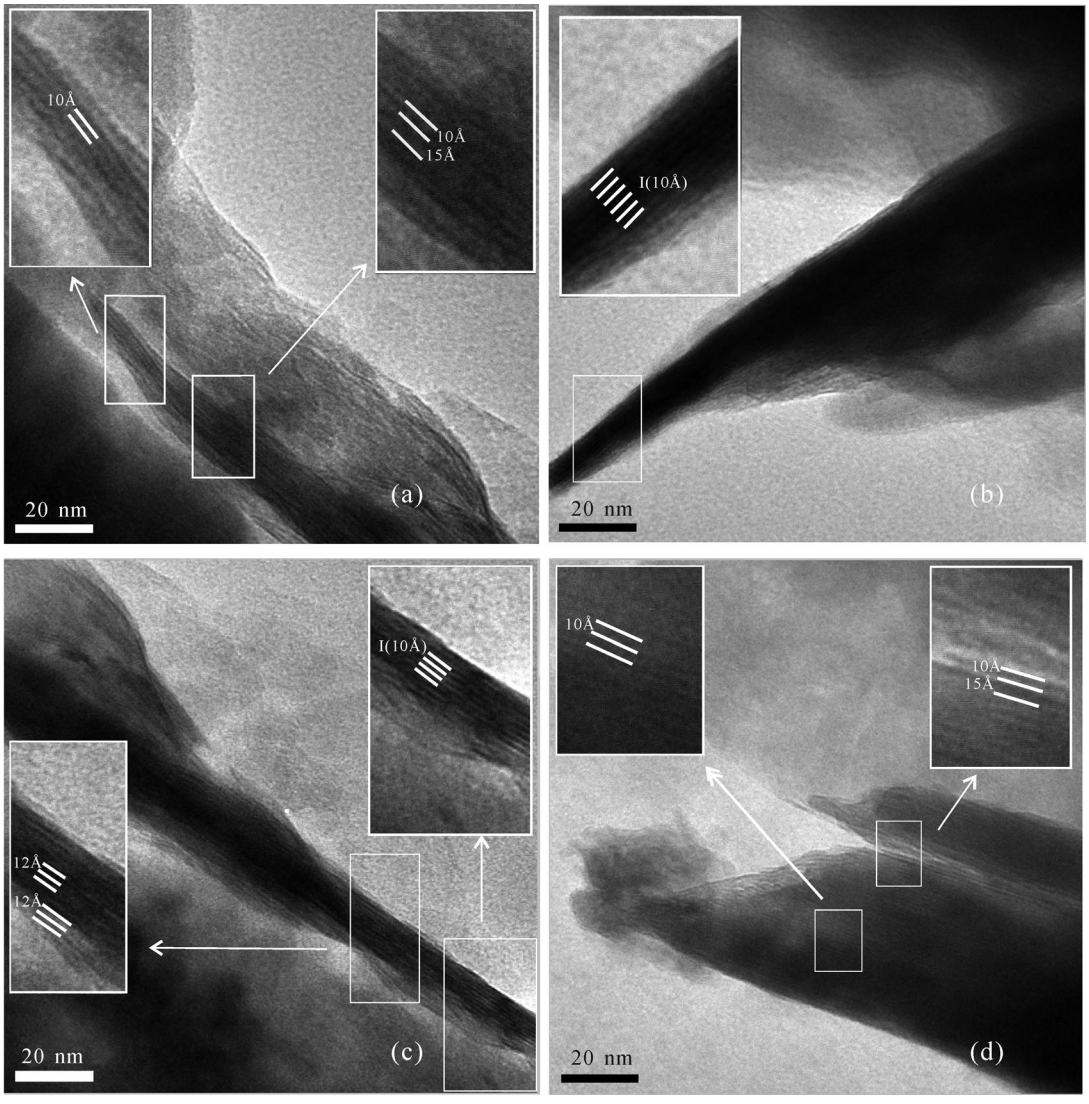

Fig. 6 HRTEM images of the Luochuan palaeosol (LC405). (a) Illite and mixed-layer illite/smectite; (b) illite mineral; (c) 15 Å smectite lattice-fringe spacing collapsed to 12 Å under the electron beam; (d) illite and mixed-layer illite/smectite.

illite interlayer: the increasing dissolution of K^+ from illite causes the increase in the IC values, and thus illite crystallinity reflects the degree of illite hydrolysis under the climate conditions (Singer, 1984; Ehrmann, 1998; Hong, 2010; Hong et al., 2012b). The IC values of the palaeosols range from 0.310° to 0.491°, while they range from 0.255° to 0.401° for the loesses. The IC values of the palaeosols are obviously larger than those of the loesses, indicating that illite in palaeosols experienced more intensive weathering or hydrolysis under relatively warm and humid climate conditions.

The relative abundance of illite in the palaeosols (64%–83%) is usually higher than in the loesses (61%–80%), consistent with the results of Zheng et al. (1985) and Ji et al. (1998). The illite chemical index of the palaeosols (0.299–0.394) is usually higher than those of the loesses (0.294–0.334), indicating that illite in palaeosols has experienced more intensive chemical weathering (hydrolysis) under relatively warm and humid climate conditions. The relative abundance of chlorite in the palaeosols (6%–21%) is notably lower than in the loesses (8%–22%), while the relative abundance of kaolinite in the palaeosols (7%–19%) is slightly larger than in the loesses (5%–18%).

The CIA values (using major element data of the Luochuan loess-palaeosols from Chen et al., 2001) of the Luochuan loess-palaeosols range from 62–69, suggesting that the chemical weathering intensity is relatively weak. However, the CIA value shows clear fluctuations in both the loess and palaeosol (Table 1). The CIA values for the loess sediments are relatively low, ranging from 62 to 65, and those of the palaeosol materials are relatively high, with values of 66–69. This also indicates that the palaeosols have experienced more intensive chemical weathering compared to the loesses. The chemical index

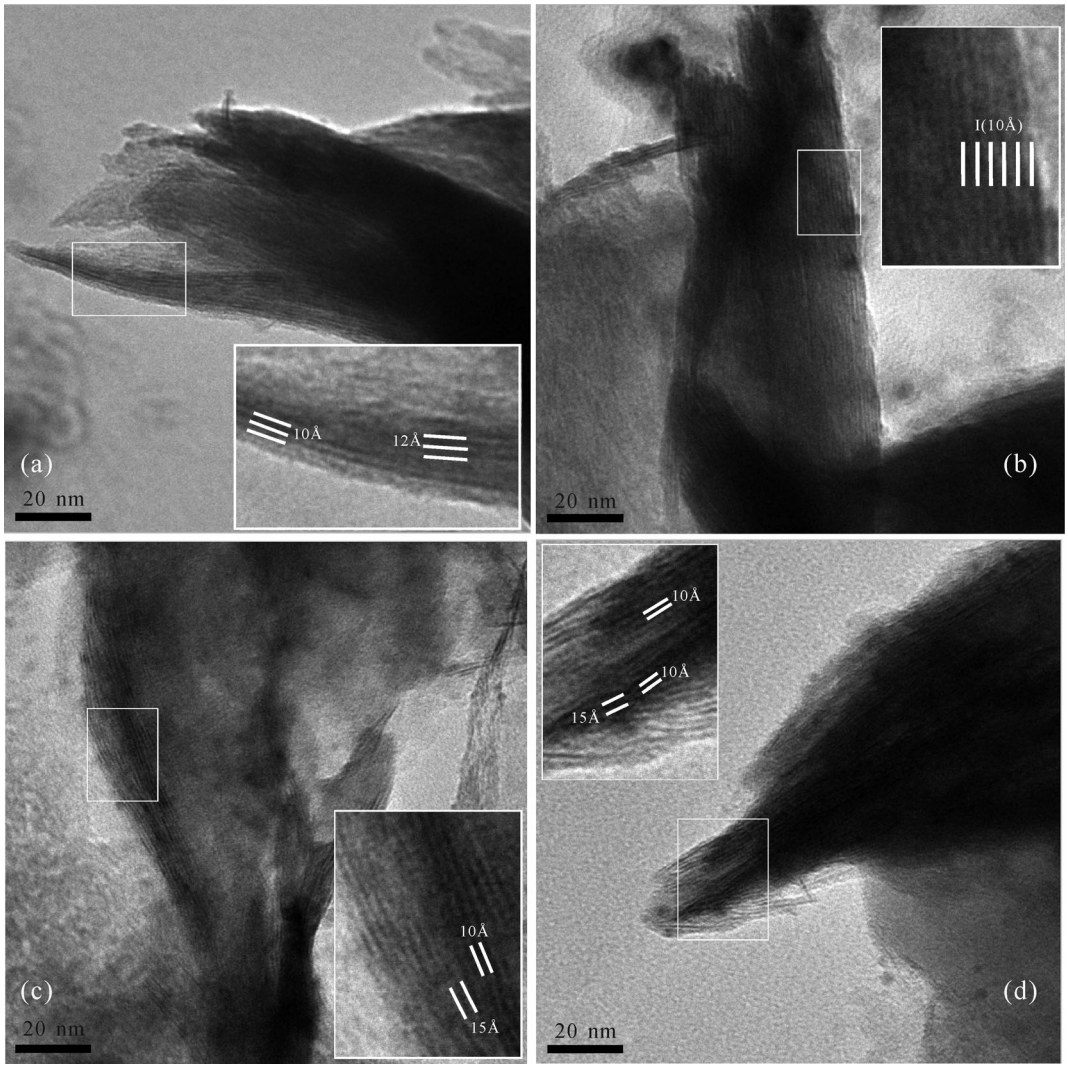

Fig. 7 HRTEM images of the Luochuan loess (LC429). (a) and (c) mixed-layer illite/smectite; (b) illite mineral; (d) illite and mixed-layer illite/smectite.

of alteration ($CIA = Al_2O_3/(Al_2O_3 + Na_2O + CaO + K_2O)$) is often used to estimate the chemical weathering intensity, which reflects the weathering of feldspar to clay minerals, and feldspar, illite, and kaolinite have CIA values of 50, 80, and 100, respectively (Nesbitt and Young, 1982). Because the CIA induces some uncertainties, Meunier et al. (2013) proposed another approach based on the M^+-4Si-R^{2+} system (where $M^+ = Na^+ + K^+ + 2Ca^{2+}$; $4Si = Si/4$; $R^{2+} = Fe^{2+} + Mg^{2+}$) that takes silica into account. The M^+-4Si-R^{2+} system is currently used to represent the composition of clay mineral assemblages formed in different water-rock interaction systems such as soils, weathered rocks, and diagenetic or hydrothermal series. In the coordinate system, the weathered granitic, mafic, and ultramafic rocks clearly show separate trends; all converge toward the 4Si pole (the chemical composition of kaolinite). The weathering intensity scale (WIS) is estimated from the co-variation of the Δ4Si % parameter and the $R^{3+}/(R^{3+} + R^{2+} + M^+)$ value (Meunier et al., 2013). The $R^{3+}/(R^{3+} + R^{2+} + M^+)$ values of the Luochuan loess-palaeosols range from 0.508 to 0.589, suggesting that the parent rocks of the Luochuan sediments are felsic. In the M^+-4Si-R^{2+} triangle diagram and the $R^{3+}/(R^{3+} + R^{2+} + M^+)$ coordinate (Fig. 8), the compositions of the Luochuan loess-palaeosols are clearly different from that of the UCC, reflecting that the loess-palaeosols have experienced a certain degree of chemical weathering. As shown in Table 1 and Fig. 4, the change in chemical weathering intensity along the Luochuan profile is in good agreement with changes in the illite crystallinity and the illite chemical index, indicating that weathering or hydrolysis characteristics of illite in the loess-palaeosol sediments are indicative of the climate conditions. Both the CIA and WIS values of the Luochuan deposits suggest that chemical weathering occurred in the materials, and transformation between clay minerals would be expected, as also confirmed by

Table 1 The calculated parameters for chemical weathering

Layer	ICI	IC	CIA%	4Si%	M^{+}%	R^{2+}%	Rat	Δ4Si%
L1	0.301	0.294	61.905	64.319	23.596	12.085	0.508	40.729
S1	0.331	0.371	66.216	65.988	21.490	12.522	0.555	43.502
L2	0.312	0.355	62.574	63.922	23.375	12.703	0.513	40.070
S2	0.324	0.322	68.498	65.101	20.460	14.439	0.566	42.028
L3	0.302	0.317	62.853	64.259	23.016	12.725	0.515	40.629
S3	0.313	0.344	66.312	65.452	21.496	13.051	0.547	42.612
L4	0.308	0.299	63.006	64.935	22.511	12.554	0.521	41.753
S4	0.320	0.341	65.946	66.694	21.441	11.866	0.555	44.674
L5	0.301	0.306	63.634	64.097	22.720	13.183	0.521	40.360
S5	0.318	0.385	69.022	68.292	19.233	12.475	0.589	47.330
L6	0.307	0.333	63.808	64.504	22.323	13.173	0.522	41.037
S6	0.324	0.398	68.651	66.364	19.872	13.763	0.568	44.127
L8	0.323	0.255	64.653	64.015	22.558	13.426	0.525	40.225
S8	0.307	0.326	66.591	65.923	21.124	12.952	0.557	43.394
L9	0.314	0.313	62.528	65.238	22.554	12.208	0.515	42.255
S9	0.334	0.483	66.704	64.798	21.131	14.071	0.553	41.525
L10	0.294	0.370	64.710	64.022	22.535	13.443	0.529	40.236
S10	0.339	0.491	66.963	64.072	21.180	14.748	0.546	40.319
L13	0.308	0.398	64.305	65.808	21.250	12.942	0.526	43.203
S13	0.344	0.445	67.482	66.434	20.229	13.337	0.560	44.242
L15	0.323	0.366	62.869	66.907	21.500	11.593	0.520	45.028

Rat: $R^{3+}/(R^{3+}+R^{2+}+M^{+})$; ICI: Illite chemical index; IC: Illite crystallinity.

HRTEM observation. Therefore, the variation of clay mineral composition between the palaeosols and the loesses of the Luochuan section corresponds well with the climate conditions during the different periods.

The Luochuan section provides a continuous record of the East Asian monsoon, as expected. The East Asian monsoon plays a crucial role in the global climate system, and has attracted wide interest because of its control on precipitation and potential influences on global climate (Schatz et al., 2015; Sun et al., 2016). Loess formed during glacial periods that were characterized by weakened summer-monsoon and strengthened winter-monsoon circulation, while paleosols developed during interglacial periods with decreased winter-monsoon intensity and intensified summer-monsoon (Sun et al., 2016).

The clay mineral composition of the Luochuan loess-palaeosols is dominated by illite (62 wt%–90 wt%), indicating a continuous cool and dry climate since 1.3 Ma. This result is confirmed by the medium CIA values (67–84), which reflect a moderate degree of weathering. The stratigraphic variation of the clay minerals implies a pattern of a general cooling and drying of the Luochuan region. The illite profile show a gradual increase from the bottom to the top of the Luochuan section; the average content of illite in the lower part (Layers S_{15}–L_{10}), middle part (Layers S_9–L_5), and upper part (Layers S_4–L_0) of the section is 74%, 74%, and 75%, respectively. The kaolinite profile, on the contrary, exhibits a gradual decrease from the bottom to the top of the Luochuan section. The average content of kaolinite in the Layers S_{15}–L_{10} is 12 wt%, and it decreases to 11 wt% in the Layers S_9–L_5 and also in the Layer S_4–L_0. The profiles of other clay minerals (chlorite and smectite) confirm the same climate trend since 1.3 Ma (Fig. 4). In addition, changes in relative proportions of clay minerals are consistent with the trends of CIA, ICI, and IC. However, during the period the profiles of all the proxies show frequent fluctuations between palaeosols and loesses along the section. Within the Luochuan section, the illite content in loess layers (average of 83%) is more than in palaeosol layers (average of 81%), indicating that the palaeosols experienced relatively stronger weathering during that time. The fluctuations of the clay minerals correspond well with the variations of CIA values, magnetic susceptibility values, and the amplitude fluctuation in oxygen isotope composition (Fig. 4), suggesting that climate changes in the Luochuan region were controlled by the global climate changes.

6 Conclusions

The clay minerals in the Luochuan loess-palaeosols are mainly illite, with minor chlorite, kaolinite, smectite, and illite-smectite mixed-layer clays. However, transformation of illite to illite-smectite was observed by HRTEM in both the loess and palaeosol in the section. The illite is the $2M_1$ polytype in structure, with a Kübler index of 0.255°–0.491°, and the illite chemical index ranges from 0.294 to 0.394. The CIA values of the loess-palaeosols range from 61.9 to 69.02, and the $R^{3+}/(R^{3+}+R^{2+}+M^{+})$ values range from 0.508 to 0.589. These suggest that the Luochuan loess-palaeosols experienced a certain degree of chemical weathering, especially the palaeosols, as indicated by HRTEM observation.

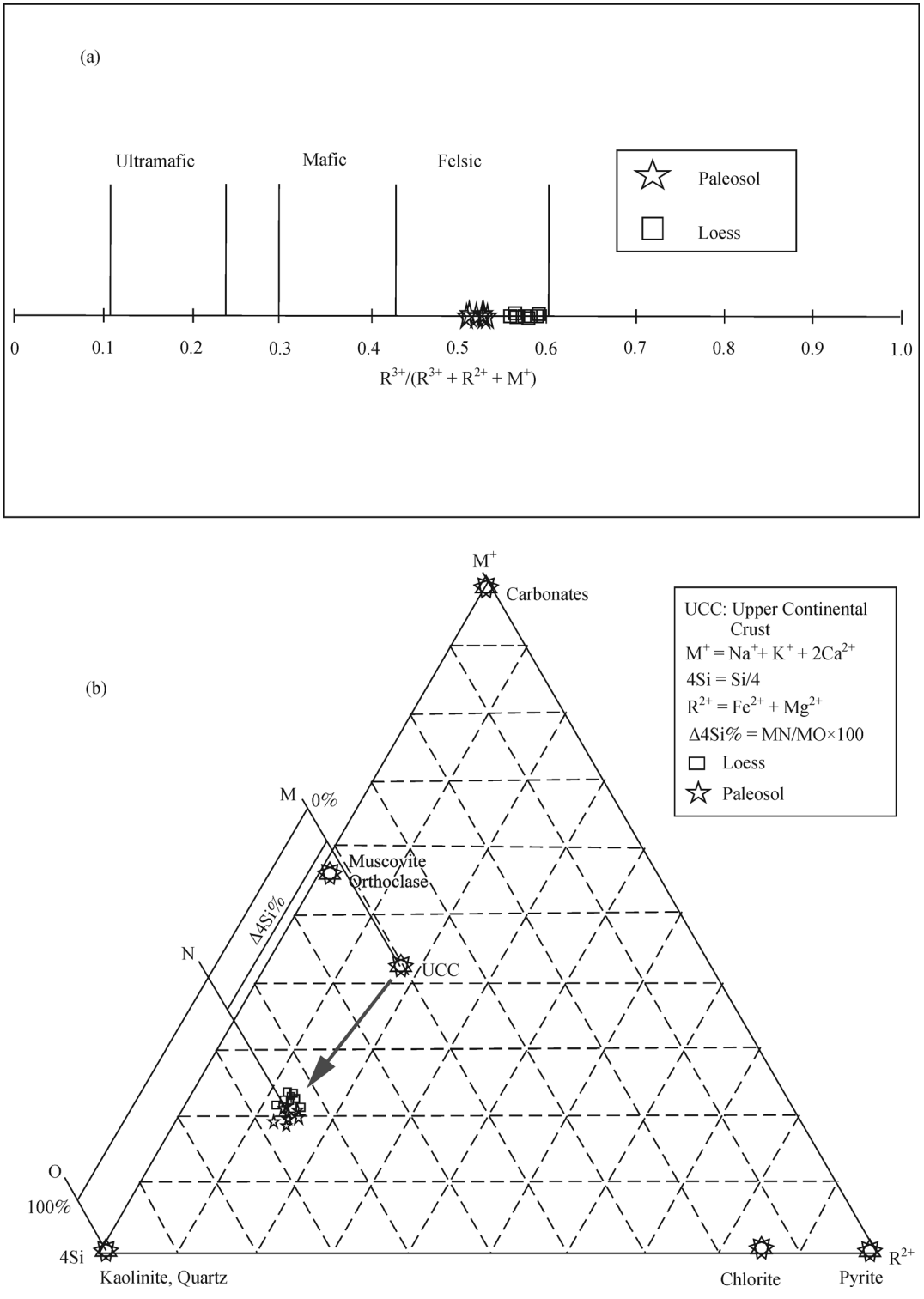

Fig. 8 (a) The representative domains of the major rock groups as scaled in the $R^{3+}/(R^{3+} + R^{2+} + M^{+})$ coordinate; (b) chemical compositions of Luochuan sediments plotted in the M^{+}-4Si-R^{2+} system.

Although the Luochuan loess-palaeosols have the same clay mineral assemblage, the relative proportions of clay minerals changed frequently along the profile, which are consistent with those of the CIA, ICI, and IC. Palaeoclimate changes suggested by the clay index are consistent with variations in the deep-sea $\delta^{18}O$ records and the

magnetic susceptibility value, indicating that climate changes in the Luochuan region were controlled by global climate changes.

Acknowledgements This work was supported by the National Natural Science Foundation of China (Grant Nos. 41272053 and 41472041). C.W. acknowledges a postdoctoral science foundation of China (2015M582301), Fundamental Research Funds for the Central Universities, China University of Geosciences (Wuhan), and National Natural Science Youth Foundation of China (Grant No. 41602037). The authors wish to thank Dr. Yu J. S. for XRD analysis, Dr. Liu X. W. for HRTEM analysis and Dr. Yang H. and Dr. Yang Q. for SEM analysis.

References

Ahmad I, Chandra R (2013). Geochemistry of loess-paleosol sediments of Kashmir Valley, India: provenance and weathering. J Asian Earth Sci, 66: 73–89

Andreola F, Castellini E, Manfredini T, Romagnoli M (2004). The role of sodium hexametaphosphate in the dissolution process of kaolinite and kaolin. J Eur Ceram Soc, 24(7): 2113–2124

Biscaye P E (1965). Mineralogy and sedimentation of recent deep-sea clay in the Atlantic Ocean and adjacent seas and oceans. Geol Soc Am Bull, 76(7): 803–832

Buggle B, Glaser B, Hambach U, Gerasimenko N, Markovic S (2011). An evaluation of geochemical weathering indices in loess-paleosol studies. Quat Int, 240(1–2): 12–21

Buggle B, Hambach U, Muller K, Zoller L, Markovic S B, Glaser B (2014). Iron mineralogical proxies and Quaternary climate change in SE-European loess–paleosol sequences. Catena, 117: 4–22

Burt R (2004). Soil survey laboratory methods manual. Soil Survey Investigations Report, 42: 735

Chen J, An Z, Liu L, Li J, Yang J, Chen Y (2001). Variation of dust chemical composition in Loess Plateau and chemical weathering of Asia inland after 2.5 Ma B.P. Sci China Earth Sci, 31(2): 136–145

Chen L, Zhang L, Wang H, Zhou L, Chen J, Yuan B (2004). Illite of ambigenous type in Luochuan Loess Section. Chin Sci Bull, 49(23): 2449–2454 (in Chinese)

Ehrmann W (1998). Implications of late Eocene to early Miocene clay mineral assemblages in McMurdo Sound (Ross Sea, Antarctica) on palaeoclimate and ice dynamics. Palaeogeogr Palaeoclimatol Palaeoecol, 139(3–4): 213–231

Gingele F X, De Deckker P, Hillenbrand C D (2001). Clay mineral distribution in surface sediments between Indonesia and NW Australia: source and transport by ocean currents. Deep-sea Geology, 179(3–4): 135–146

Hallam A, Grose J A, Ruffell A H (1991). Palaeoclimatic significance of changes in clay mineralogy across the Jurassic-Cretaceous boundary in England and France. Palaeogeogr Palaeoclimatol Palaeoecol, 81 (3–4): 173–187

Hong H L (2010). A review on palaeoclimate interpretation of clay minerals. Geological Science and Technology Information, 29(1): 1–8 (in Chinese)

Hong H L, Du D, Li R, Churchman J G, Yin K, Wang C (2012a). Mixed-layer clay minerals in the Xuancheng red clay sediments, Xuancheng, Anhui Province. Earth Science-Journal of China University of Geosciences, 37(3): 424–432 (in Chinese)

Hong H L, Li Z, Xue H J, Zhu Y H, Zhang K X, Xiang S Y (2007). Oligocene clay mineralogy of the Linxia basin: evidence of palaeoclimatic evolution subsequent to the initial-stage uplift of the Tibetan plateau. Clays Clay Miner, 55(5): 491–505

Hong H L, Wang C, Zheng K, Zhang K, Yin K, Li Z (2012b). Clay mineralogy of the Zhada sediments: evidence for climatic and tectonic evolution since ~9 Ma in Zhada, Southwestern Tibet. Clays Clay Miner, 60(3): 240–253

Hong H L, Zhang N, Li Z, Xue H, Xia W, Yu N (2008). Clay mineralogy across the P-T boundary of the Xiakou section, China: evidence of clay provenance and environment. Clays Clay Miner, 56(2): 131–143

Hu P, Liu Q, Torrent J, Barron V, Jin C (2013). Characterizing and quantifying iron oxides in Chinese loess/paleosols: implications for pedogenesis. Earth Planet Sci Lett, 369–370: 271–283

Jaramillo S S, Mccarthy P J, Trainor T P, Fowell S J, Fiorillo A R (2015). Origin of clay minerals in alluvial palaeosols, Prince Creek formation, North slope, Alaska U.S.A: influence of volcanic ash on pedogenesis in the late Cretaceous Arctic. J Sediment Res, 85(2): 192–208

Ji J, Chen J, Liu L, Lu H (1999). Chemical weathering and magnetic susceptibility increase of chlorite in Luochuan loess. Prog Nat Sci, 9 (7): 619–623 (in Chinese)

Ji J, Chen J, Lu H (1998). Transmission electron microscopy evidence of illite origin in Luochuan loess, Shaanxi. Chin Sci Bull, 43(19): 2095–2098 (inChinese)

Ji J, Chen J, Wang H (1997). Crystallinity of illite from the Luochuan Loess-Palaeosol sequence, Shaanxi Province. Geological Review, 43 (2): 181–185 (in Chinese)

Keller W D (1970). Environmental aspects of clay minerals. J Sediment Petrol, 40(3): 788–854

Kisch H J (1991). Illite crystallinity: recommendations on sample preparation, X-ray diffraction settings, and interlaboratory samples. J Metamorph Geol, 9(6): 665–670

Li Y, Song Y, Chen X, Li J, Mamadjanov Y, Aminov J (2016). Geochemical composition of Tajikistan loess and its provenance implications. Palaeogeogr Palaeoclimatol Palaeoecol, 446: 186–194

Lu H, An Z, Liu H, Yang W (1998). Periodicity of east Asian winter and summer monsoon variation during the past 2500 ka recorded by loess deposits at Luochuan on the central Chinese loess plateau. Geological Review, 44(5): 553–558 (in Chinese)

Lu S, Wang S, Chen Y (2015). Palaeopedogenesis of red palaeosols in Yunnan Plateau, southwestern China: pedogenical, geochemical and mineralogical evidences and palaeoenvironmental implication. Palaeogeogr Palaeoclimatol Palaeoecol, 420: 35–48

Lu Y, Sun J, Li P (2008). Predicting palaeoclimate since 140 Ma B.P. by experiment of carbon isotope in loess. Ganhanqu Ziyuan Yu Huanjing, 22(1): 60–63 (in Chinese)

Meunier A, Caner L, Hubert F, El Albani A, Prét D (2013). The weathering intensity Scale(WIS): an alternative approach of the chemical index of alteration (CIA). Am J Sci, 313(2): 113–143

Nesbitt H W, Young G M (1982). Early Proterozoic climates and plate motions inferred from major element chemistry of lutites. Nature, 299 (5885): 715–717

Nieto F, Ortega-Huertas M, Peacor D R, Arostegui J (1996). Evolution of illite/smectite from early diagenesis through incipient metamorph-

ism in sediments of the Basque-Cantabrian Basin. Clays Clay Miner, 44(3): 304–323

Perederij V I (2001). Clay mineral composition and palaeoclimatic interpretation of the Pleistocene deposits of Ukraine. Quat Int, 76–77: 113–121

Petschick R, Kuhn G, Gingele F (1996). Clay mineral distribution in surface sediments of the South Atlantic: sources, transport, and relation to oceanography. Deep-sea Geology, 130: 203–229

Rao W, Li X, Gao Z, Luo T (2004). Distribution of fixed-NH_4^+-N in Luochuan loess section. J Desert Res, 24(6): 685–688 (in Chinese)

Rateev M A, Gorbunova Z N, Lisitzyn A P, Nosov G L (1969). The distribution of clay minerals in the oceans. Sedimentology, 13(1–2): 21–43

Schatz A, Scholten T, Kühn P (2015). Paleoclimate and weathering of the Tokaj (Hungary) loess–paleosol sequence. Palaeogeogr Palaeoclimatol Palaeoecol, 426: 170–182

Singer A (1984). The Palaeoclimatic interpretation of clay minerals in sediment—A review. Earth Sci Rev, 21(4): 251–293

Sun J, Liu T (2002). Pedostratigraphic subdivision of the loess-palaeosol sequences at Luochuan and a new interpretation on the palaeoenvironmental significance of L9 And L15. Quaternary Sciences, 22(5): 406–412 (in Chinese)

Sun Y, Kutzbach J, An Z, Clemens S, Liu Z, Liu W, Liu X, Shi Z, Zheng W, Liang L, Yan Y, Li Y (2015). Astronomical and glacial forcing of East Asian summer monsoon variability. Quat Sci Rev, 115: 132–142

Sun Z, Owens P R, Han C, Chen H, Wang X, Wang Q (2016). A quantitative reconstruction of a loess–paleosol sequence focused on paleosol genesis: an example from a section at Chaoyang, China. Geoderma, 266: 25–39

Terhorst B, Kuhn P, Damm B, Hambach U, Meyer-Heintze S, Sedov S (2014). Paleoenvironmental fluctuations as recorded in the loess-paleosol sequence of the Upper Paleolithic site Krems-Wachtberg. Quat Int, 351: 67–82

Trindade M J, Rocha F, Dias M I, Prudêncio M I (2013). Mineralogy and grain-size distribution of clay-rich rock units of the Algarve Basin (South Portugal). Clay Miner, 48(1): 59–83

Wang H, Zhou J (1998). On the indices of illite crystallinity. Acta Petrologica Sinica, 14(3): 395–405 (in Chinese)

Xie Q, Chen T, Sun Y, Li X, Xu X (2008). Composition of ferric oxides in the Luochuan loess-red clay sequences on China's loess plateau and its palaeoclimatic implications. Acta Mineralogica Sinica, 28(4): 389–396 (in Chinese)

Xu Y, Hong H, He Y (2010). Clay mineralogy and its geological significance of sediments in the foreland basin of West Kunlun Mountains. Acta Sedimentologica Sinica, 28(4): 659–668 (in Chinese)

Yang H, Pancost R D, Tang C, Ding W, Dang X, Xie S (2014). Distributions of isoprenoid and branched glycerol dialkanol diethers in Chinese surface soils and a loess–paleosol sequence: implications for the degradation of tetraether lipids. Org Geochem, 66: 70–79

Yang M, Zhang H, Lei G, Zhang W, Fan H, Chang F, Niu J, Chen Y (2006). Biomarkers in weakly developed palaeosol (L_1SS_1) in the Luochuan loess section and reconstructed palaeovegetation-environment during the interstade of the last glaciation. Quaternary Sciences, 26(6): 976–984 (in Chinese)

Yuan B, Ba T, Cui J, Yin Q (1987). The relationship between gully development and climatic changes in the loess Yuan region: examples from Luochuan, Shaanxi Province. Acta Geogr Sin, 42 (4): 328–337 (in Chinese)

Zhang H, Yang M, Zhang W, Lei G, Chang F, Pu Y, Fan H (2007). Diversification of biomarkers and vegetation of S4 palaeosol and the adjacency loess in the Luochuan loess section. Sci China Earth Sci, 37(12): 1634–1642 (in Chinese)

Zheng H, Gu X, Han J, Deng B (1985). Clay minerals in loess of China and their tendency in loess section. Quaternary Sciences, 6(1): 158–165 (in Chinese)